Supporting Information

Side-chain engineering for high degradation performance of mandrel materials in ICF target fabrication

Yu Zhu[#,a], Qiang Chen[#,b], Chaoyang Wang[b], Yue Xin[a], Lu Wang[a], Yong Yi[c], Zhanwen Zhang[b], Yongjian Tang*[,b,c], and Zhigang Wang*[,a,d]

a Institute of Atomic and Molecular Physics, Jilin University, Changchun 130012, China

b Laser Fusion Research Center, China Academy of Engineering Physics, Mianyang 621900, China

c State Key Laboratory of Environmental-friendly Energy Materials, School of Material Science and Engineering, Southwest University of Science and Technology, Mianyang 621010, China

d College of Physics, Jilin University, Changchun 130012, China

# Authors contributed equally

* Correspondence email: tangyongjian2000@sina.com (Y. T.); wangzg@jlu.edu.cn (Z. W.)

Part 1. B1 diagnostics.

Part 2. Reaction rate calculation.

Part 3. The relative energies between the different isomers of chain structures.

Part 4. Bond properties of C-C bonds on the main chain of different chain structures.

Part 5. Spin population of different structures.

Part 6. The degradation reactions related to the tail end of structures.

Part 7. The EDA between the first monomer and the remaining fragments in different structures.

Part 8. The frontier molecular orbitals of different structures.

Part 1. B1 diagnostics.

B_1 diagnosis is an effective method to measure the multireference characters of systems[1-3], which can be defined as:

$$B_1 = (BE_{BLYP} - BE_{B1LYP//BLYP})/n$$

where, BE_{BLYP} and $BE_{B1LYP//BLYP}$ are the bond energies computed with BLYP and B1LYP//BLYP, n is the number of bonds being broken. If the value (divided by 1 kcal/mol to produce a unitless diagnostic) of B_1 diagnostic exceeds 10.0, the multireference methods should be considered.

Table S1. The B_1 values of different structures.

	PAMS	R1	R2-1	R2-2	R3-1	R3-2	R4-1	R4-2	R4-3	R4-4
B_1 Values	4.15	3.00	4.38	3.46	4.15	3.23	4.38	4.38	3.92	3.69

Part 2. Reaction rate calculation.

Reaction rate constants were also calculated in terms of the transition state theory (TST) with Eckart Tunneling corrections[4,5]. The equation presented for the conventional TST is:

$$k^{TST}(T) = \sigma\frac{k_bT}{h}(\frac{RT}{P^0})^{\Delta n}e^{\frac{-\Delta G^{\neq,0}(T)}{k_bT}}$$

where σ is the reaction path degeneracy, k_b is the Boltzmann's constant, T is the temperature, h is the Planck's constant, R is the ideal gas constant, P^0 is the pressure, $\Delta G^{\neq,0}(T)$ represents the standard Gibbs free energy ($\Delta n = 1$ for gas-phase bimolecular). If the tunneling corrections are considered, then $k^{TST}/_T(T)$= χ(T) × $k^{TST}(T)$. Where χ(T) is transmission coefficient. As for Eckart correction, then

$$\chi(\mathrm{T}) = \frac{e^{\frac{\Delta H_f^{\pm,0K}}{k_bT}}}{k_bT}\int_0^{\infty} p(E)e^{-\frac{E}{k_bT}}\,\mathrm{dE}$$

Where $p(E) = 1 - [\frac{cosh[2\pi(\alpha-\beta)+cosh[2\pi\delta]}{cosh[2\pi(\alpha+\beta)+cosh[2\pi\delta]}]$,

$$\alpha = \frac{1}{2\sqrt{C}}\sqrt{E} \qquad \beta = \frac{1}{2\sqrt{C}}\sqrt{E-A} \qquad \delta = \frac{1}{2\sqrt{C}}\sqrt{E-B}$$

$$A = \Delta H_f^{\pm,0K} - \Delta H_r^{\pm,0K} \qquad B = (\sqrt{\Delta H_f^{\pm,0K}} - \sqrt{\Delta H_r^{\pm,0K}})^2$$

$$C = (hIm(v^{\neq}))^2[\frac{B^3}{A^2-B^2}]^2$$

$\Delta H_f^{\pm,0K}$,$\Delta H_r^{\pm,0K}$ represent the zero-point corrected energy barriers in the reverse and forward direction, $Im(v^{\neq})$ is the imaginary frequency.

Part 3. The relative energies between the different isomers of chain structures.

Table S2. The relative energies between the different isomers of the structures with cyclopentadiene, naphthalene or azulene as the side chain.

	R2-1	R2-2	R3-1	R3-2	R4-1	R4-2	R4-3	R4-4
ΔE (eV)	0	1.73	0	1.18	0	0.66	1.02	2.08

Part 4. Bond properties of C-C bonds on the main chain of different chain structures.

Table S3. Bond lengths and bond orders of C-C bonds (a-g) on the main chain of different chain structures. The specific location can be seen in schematic diagram.

	Bond Length (Å)/Bond Order						
	a	**b**	**c**	**d**	**e**	**f**	**g**
PAMS	1.51/1.03	1.59/0.94	1.56/0.97	1.57/0.96	1.57/0.96	1.57/0.97	1.51/0.98
R1	1.50/1.06	1.60/0.92	1.58/0.97	1.58/0.97	1.59/0.95	1.58/0.97	1.51/0.99
R2-1	1.50/1.02	1.59/0.93	1.56/0.96	1.57/0.96	1.57/0.96	1.57/0.97	1.51/0.99
R2-2	1.50/1.06	1.58/0.94	1.57/0.97	1.58/0.95	1.57/0.96	1.57/0.98	1.51/0.98
R3-1	1.51/1.03	1.59/0.93	1.56/0.96	1.57/0.96	1.57/0.96	1.57/0.97	1.51/0.99
R3-2	1.51/1.02	1.59/0.94	1.57/0.97	1.58/0.96	1.58/0.96	1.58/0.96	1.51/0.98
R4-1	1.51/1.02	1.59/0.94	1.56/0.97	1.57/0.96	1.57/0.96	1.56/0.98	1.51/0.99
R4-2	1.51/1.01	1.59/0.93	1.57/0.96	1.57/0.95	1.58/0.96	1.57/0.96	1.51/0.98
R4-3	1.51/1.02	1.59/0.93	1.57/0.96	1.57/0.96	1.58/0.96	1.58/0.96	1.51/0.98
R4-4	1.51/1.02	1.59/0.93	1.57/0.96	1.58/0.96	1.58/0.96	1.58/0.97	1.52/0.98

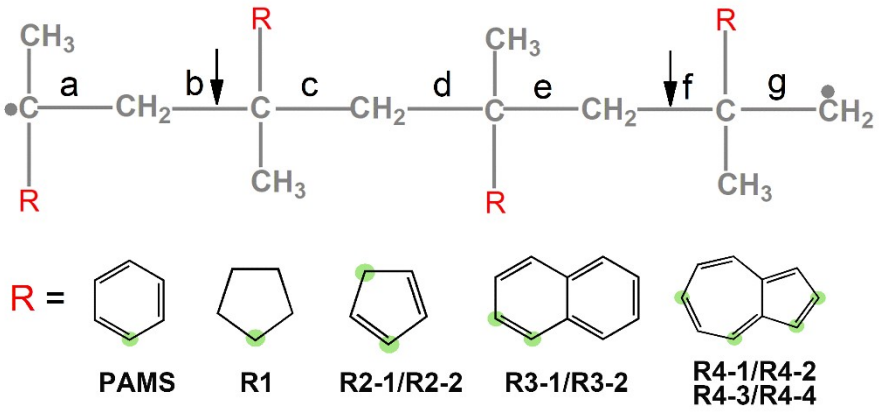

Schematic diagram. Geometric images of structures with different hydrocarbon cyclic

functional groups as the side chain. The grey letters indicate the C-C bonds on the main chain. The black dots represent unpaired electrons. Light green shading represents different substitution sites.

Part 5. Spin population of different structures.

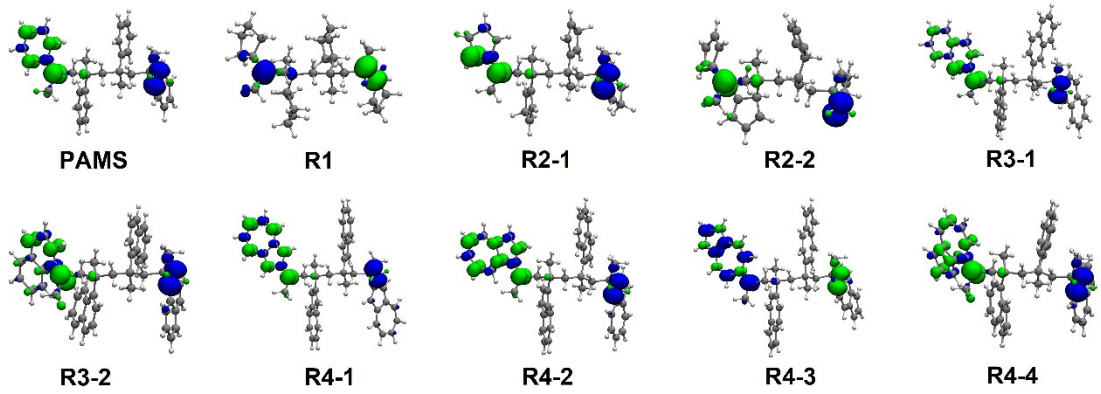

Fig. S1. Spin population of structures with different side chains. The blue and green areas on structures represent the net spin up and down, respectively. Isovalue = 0.005.

Part 6. The degradation reactions related to the tail end of structures.

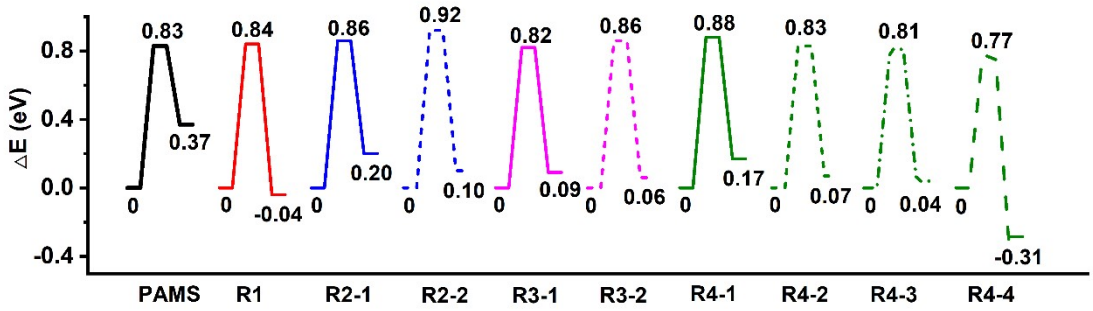

Fig. S2. Potential energy surfaces (PESs) of degradation reactions related to the tail end of structures. These reactions all generate the monomer. The left and right side of each PESs represent the reactant and product. The energy of the reactant in each reaction is taken as the zero.

Table S4. The energy barriers of head-end and tail-end depolymerization (D_{head} and D_{tail}) reactions for different ring substitution structures. The unit is eV.

	PAMS	R1	R2-1	R2-2	R3-1	R3-2	R4-1	R4-2	R4-3	R4-4
D_{head}	0.72	0.52	0.72	0.70	0.69	0.58	0.72	0.76	0.69	0.63
D_{tail}	0.83	0.84	0.86	0.92	0.82	0.86	0.88	0.83	0.81	0.77

Part 7. The EDA between the first monomer and the remaining fragments in different structures.

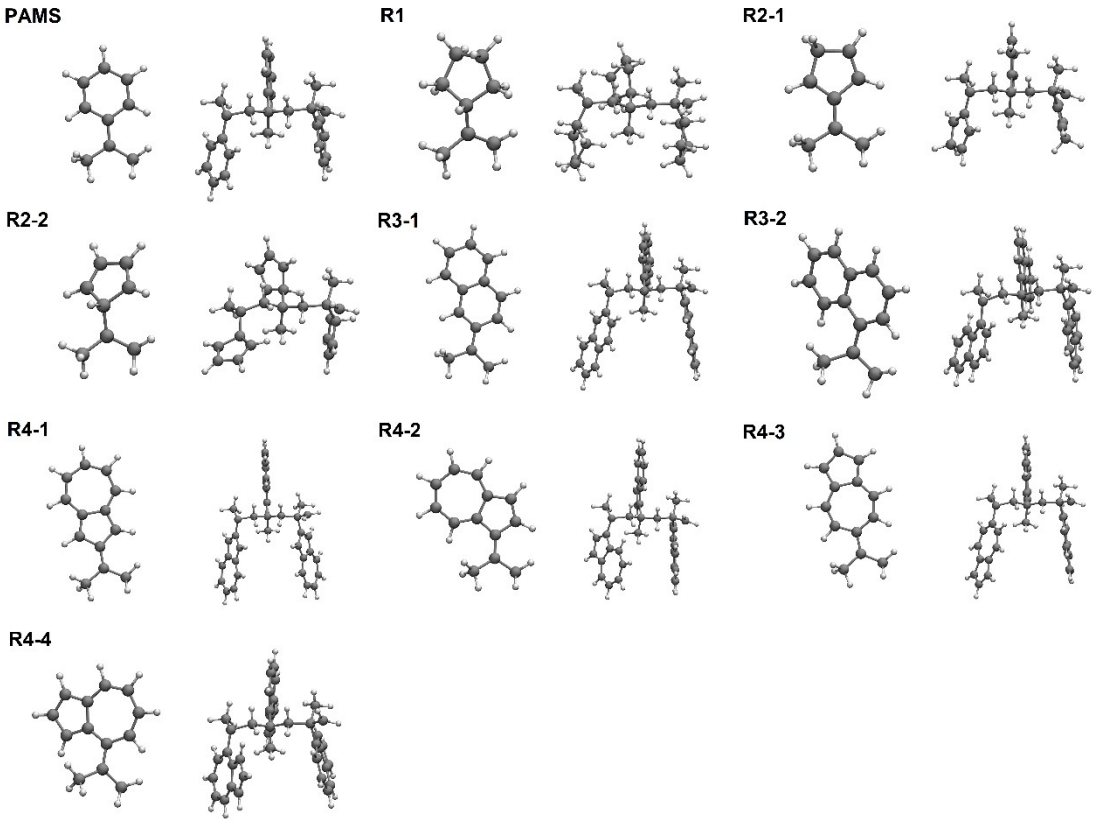

Fig. S3 The fragments used for the EDA of different structures. For each structure, the head-end monomer (left) and the rest in the structure (right) are divided into two fragments.

Table S5. The EDA between the first monomer and the remaining fragments in different chain structures. The unit of energy is eV. The values in parentheses represent the ratios of different interaction energies to the total attractive interaction energies.

	E_{orb}	E_{elstat}	E_{disp}	E_{pauli}	E_{int}
PAMS	-11.18	-7.13	-0.48	14.70	-4.09
	(59.50%)	(37.92%)	(2.58%)		
R1	-10.88	-7.09	-0.48	14.50	-3.95
	(58.98%)	(38.42%)	(2.60%)		
R2-1	-11.24	-7.14	-0.46	14.72	-4.11
	(59.68%)	(37.90%)	(2.42%)		
R2-2	-11.38	-7.14	-0.57	14.78	-4.30
	(59.61%)	(37.41%)	(2.98%)		
R3-1	-11.17	-7.13	-0.50	14.73	-4.08
	(59.38%)	(37.94%)	(2.68%)		
R3-2	-11.21	-7.27	-0.70	15.08	-4.10
	(58.44%)	(37.92%)	(3.64%)		
R4-1	-11.09	-6.91	-0.48	14.35	-4.13
	(60.03%)	(37.37%)	(2.60%)		
R4-2	-11.43	-7.54	-0.54	15.41	-4.11
	(58.57%)	(38.65%)	(2.78%)		
R4-3	-11.18	-6.87	-0.52	14.34	-4.24
	(60.19%)	(37.00%)	(2.80%)		
R4-4	-11.24	-6.98	-0.62	14.63	-4.21
	(59.64%)	(37.04%)	(3.32%)		

Part 8. The frontier molecular orbitals of different structures.

As can be seen from Fig. S4 below, the frontier MOs of different structures are all not only distributed on unsaturated carbon atoms, but delocalize to adjacent cyclic functional groups. But the degree of delocalization of these orbitals of different structures is different. Taking the HOMO-α as an example, it is mainly distributed at the unsaturated head-end and the nearby cyclic functional groups. But the compositions of this orbital for different substituted structures are not the same.

Table S6 shows the contributions of unsaturated carbon atom and cyclic functional groups to HOMO-α. Among all the substituted structures, the unsaturated carbon atom of R1 contributes the most to the HOMO-α, while that of R4-2 contributes the least, indicating that the HOMO-α of R1 is mainly localized on the unsaturated carbon atom, while this orbital of R4-2 is more delocalized. It is worth noting that the C-C bond attached to the unsaturated carbon atoms is broken in the head-end depolymerization reaction. Thus, the orbital delocalization explains the lower energy barrier required for head-end depolymerization of R1, while the higher energy barrier required for that of R4-2.

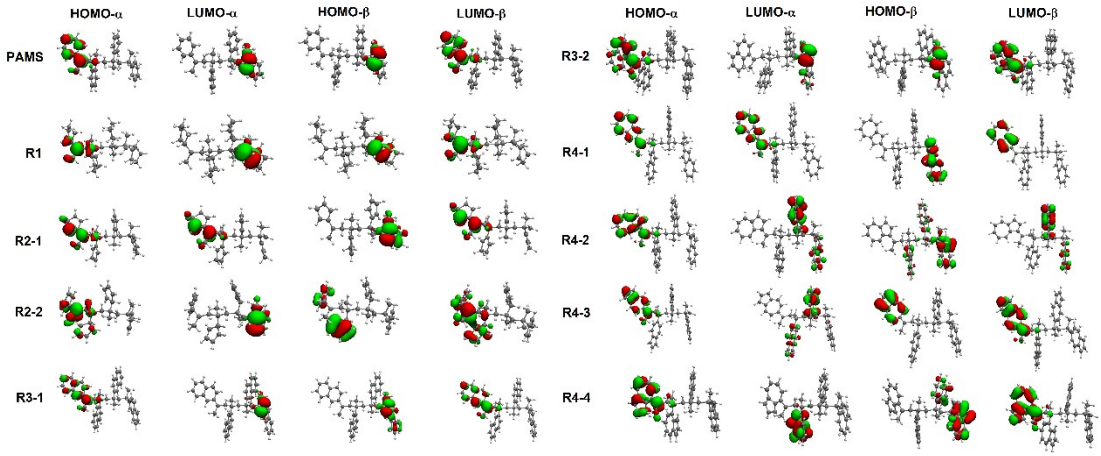

Fig. S4. The frontier molecular orbitals (MOs) of different substituted structures. Isovalue= 0.035.

Table S6. The contributions of unsaturated carbon atom and cyclic functional groups to HOMO-α.

	PAMS	R1	R2-1	R2-2	R3-1	R3-2	R4-1	R4-2	R4-3	R4-4
Unsaturated carbon atom	44.1%	66.7%	42.1%	62.6%	39.4%	41.6%	28.9%	26.1%	32.0%	30.7%
Cyclic functional groups	42.7%	10.9%	44.1%	10.8%	48.8%	46.0%	62.4%	66.3%	58.3%	57.7%

References

1. Schultz N. E.; Zhao Y.; Truhlar D. G. *J. Phys. Chem. A*, 2005, 109, 11127-11143.

2. Zheng J. J.; Zhao Y.; Truhlar D. G. *J. Phys. Chem. A*, 2007, 111, 4632-4642.

3. Galano A.; Muñoz-Rugeles L.; Alvarez-Idaboy J. R.; Bao J. L.; Truhlar D. G. *J. Phys. Chem. A*, 2016, 120, 4634−4642 .

4. Canneaux S.; Bohr F.; Henon E. *J. Comput. Chem.*, 2013, 35, 82–93.

5. Eckart C. *Phys. Rev.*, 1930, 35, 1303–1309.